

Short Communication

Development of a Graphene Oxide-ZnO Nanorod Composite for Sensitive Determination of Catecholamine

Feng Zhang and Danni Li*

Department of Neurology, Ji'nan Central Hospital Affiliated to Shandong University, Jinan, Shandong Province, 250013, P.R. China

*E-mail: zxylfzfeng@sina.com

Received: 22 December 2017 / *Accepted:* 4 February 2018 / *Published:* 6 March 2018

The present study proposed a facile hydrothermal method for the preparation of a reduced graphene oxide-ZnO (RGO-ZnO) nanorod composite. A GCE modified by this nanocomposite was used for the determination of catecholamine (CA). The proposed biosensor showed a linear dependence on the CA concentration in the range of 1 to 800 μM . The limit of detection was obtained as 0.322 μM based on the signal-to-noise ratio of 3. Furthermore, our developed biosensor proved highly stable and reproducible, with good anti-interference properties towards the detection of CA.

Keywords: Eosinophil cationic protein; Aptamer sensor; Graphene; Electrochemical determination; Childhood asthmatic attack

1. INTRODUCTION

As a type of endogenous substance in the nervous system, catecholamines (CAs) possess amine and catechol groups, mainly including dopamine (DA), epinephrine (E), and norepinephrine (NE). The clinical analysis of CAs and their metabolites has been reported, considering their significance in regulating the central and peripheral nervous systems. For example, changes in CA in the brain of Alzheimer's disease (AD) patients were investigated by Adolfsson in 1970s; in the AD patients' brains, the mean concentrations of CA and noradrenaline were greatly decreased [1-4]. Based on the study of CA and cholinergic enzymes in presenile and senile AD patients in 1983, Yates reported a significant loss of noradrenergic and cholinergic neurons in AD patients, showing decreased CA levels compared to those of the normal group [5, 6]. In recent years, Umegaki reported the metabolism of CAs in AD patients' plasmas; the results suggested the vital importance of the cholinergic system in the hippocampus for the regulation of the peripheral metabolism of CAs and inferred that the deficiency in cholinergic presynaptic neurons led to AD. Compared with the control group, the AD

patients showed much lower CAs in plasma [7, 8]. Thereafter, the close correlation of CA levels in body tissue to the diagnosis of AD has been reported in different studies [9-13]. It can be concluded that the analysis of CA levels in urine and plasma is of pivotal significance to AD diagnosis, therapy, and prognosis.

A series of chromatographic techniques have been reported for the detection of CAs in biological specimens, including high-performance liquid chromatography-mass spectrometry (HPLC-MS) [14], HPLC coupled with electrochemical (ED) or fluorescence (FL) detection [15, 16], and capillary electrophoresis (CE). The detection of low CA concentrations in biological specimens has been reported using a high-performance liquid chromatography method coupled with fluorescence detection (HPLCFL) [3, 17, 18]. The FL of CAs cannot be employed in the detection of biological specimens due to its comparative weakness. Upon the reaction with meso-1,2-diphenylethylenediamine (DPE), the CA o-dihydroxy and amino groups show enhanced detection sensitivity. Based on the literature, Yoshitake et al. proposed the detection of AD, noradrenaline, serotonin, and their metabolites using an FL method after the derivatization with benzyl amine and 1,2-DPE [19]. Umegae et al. reported the detection of CA in plasma and urine using 1,2-diarylethylenediamines as a pre-column FL derivatization reagent [20], where the biological specimens could be detected using the aforementioned methods. The present study aims to detect CAs and their metabolites in human urine. In addition, we further studied its application in the CA detection in AD.

Meanwhile, electrochemical sensors are characterized by high sensitivity, rapid detection, selectivity, low cost, and easy operation for the detection of CAs. In addition, the biosensors can also be used as miniaturized, powerful, or portable apparatuses, which can detect biomarkers of certain diseases (e.g., Parkinson's disease and Alzheimer's disease).

This work proposed the synthesis of a reduced graphene oxide-ZnO nanorods (RGO-ZnO) nanocomposite through a one-pot method. Furthermore, the fabricated RGO-ZnO nanocomposite was used for the preparation of an electrochemical biosensor for the detection of CA. Furthermore, the RGO-ZnO was characterized using a series of techniques, including X-ray diffraction (XRD) and Raman spectroscopy. Then, we studied the feasibility of the developed sensor for the CA detection using CV and potentiostatic techniques. Compared with other modified electrodes, including the bare GCE, a ZnO-modified GCE and a RGO-modified GCE, the RGO-ZnO-modified GCE exhibited a significantly lower oxidation potential and a higher current response.

2. EXPERIMENTS

Hydrazine solution (25% in water), zinc nitrate hexahydrate ($\text{Zn}(\text{NO}_3)_2 \cdot 6\text{H}_2\text{O}$), uric acid (UA), ascorbic acid (AA), glucose, 3-hydroxytyramine hydrochloride (DA), acetylcholine (Ach), and H_2O_2 were commercially available from Sigma-Aldrich. Graphene oxide powder was commercially available from JCNANO, Inc. All other test reagents were of analytical grade and were used without further purification. For the preparation of a phosphate buffer solution (PBS), a 0.1 M solution of K_2HPO_4 and KH_2PO_4 was mixed together to an appropriate pH. All the used solution was prepared using 18.2 M Ω cm Milli-Q water.

For the synthesis of RGO-ZnO, we first prepared a 1 mg/mL GO dispersion by mixing 10 mL of water with 10 mg of GO under sonication for 120 min. Afterwards, the obtained GO dispersion was gradually mixed with 10 mL of $\text{Zn}(\text{NO}_3)_2 \cdot 6\text{H}_2\text{O}$ (50 mM) and stirred for 60 h. The mixed solution was further added with 2 mL hydrazine solution (5 wt%) to obtain a grey-coloured slurry. After stirring for 60 min, it was transferred to a 30 mL Teflon-lined stainless-steel autoclave and heated for 120 min at 120 °C. The obtained samples were collected through centrifugation, followed by drying at 70 °C in an oven. The final product was named the RGO-ZnO nanocomposite.

An XRD apparatus with Cu $K\alpha$ radiation (D8-Advanced, Bruker, Germany) was used to obtain the XRD patterns (5° to 90° in 2θ). A scanning electron microscope (SEM, S-4700, Hitachi High Technologies Corporation, Japan) was used for the characterization of the surface morphology of the sample. Raman spectroscopy was carried out at ambient temperatures on a Raman Microprobe (Renishaw RM1000) laser light (514 nm). Electrochemical measurements were carried out using a GCE polished with an alumina-water slurry and then rinsed with water. The electrode was modified by dropping 8 μL of the catalyst dispersion (0.5 mg/mL) onto the surface of the GCE, followed by drying at ambient temperature. The electrochemical experiments were carried out using a CH Instruments 660A electrochemical workstation (CHI-660 A, CH Instruments, Texas, USA) with a three-electrode geometry, where the reference and auxiliary electrodes were a Ag/AgCl (3 M KCl) electrode and a platinum wire, respectively.

3. RESULTS AND DISCUSSION

Raman spectroscopy was carried out to confirm the reduction of GO under hydrothermal conditions, considering its desirable sensitivity towards the electronic structure of carbon. Both GO and RGO-ZnO showed two typical peaks at 1579 and 1340 cm^{-1} , as shown in the spectra of Fig. 1; these two peaks were indexed to the graphite (G) and diamondoid (D) bands, respectively. The D/G intensity ratio increased in the range of 0.93 to 1.12 after hydrothermal treatment, which suggested that GO was reduced and a higher concentration of defects existed in the RGO sheets [21].

GO and RGO-ZnO were further characterized by XRD, as shown in Fig. 1B. A significant peak was observed at 11.2° for GO, which resulted from the (001) lattice plane; this result can be confirmed from the previous literature [22]. These findings indicate that the ZnO nanoparticles decorated on the graphene sheets are of the hexagonal wurtzite phase with a size of 12–23 nm according to the Scherrer formula [23]. For RGO-ZnO, peaks can be observed at 31.4° , 34.2° , 35.7° , 47.4° , 56.2° , 62.5° and 67.4° in its diffractogram, which correspond to the hexagonal wurtzite ZnO (JCPDS Card 36-1451). Furthermore, for the GO, the disappearance of the diffraction peak at 11.2° and the presence of a new broad peak centred at 26.4° (002) provided additional evidence that the GO was successfully reduced under the hydrothermal conditions. It has been reported that, if the regular stacks of GO or graphite are destroyed, for example by exfoliation, their diffraction peaks become weak or may even disappear [24].

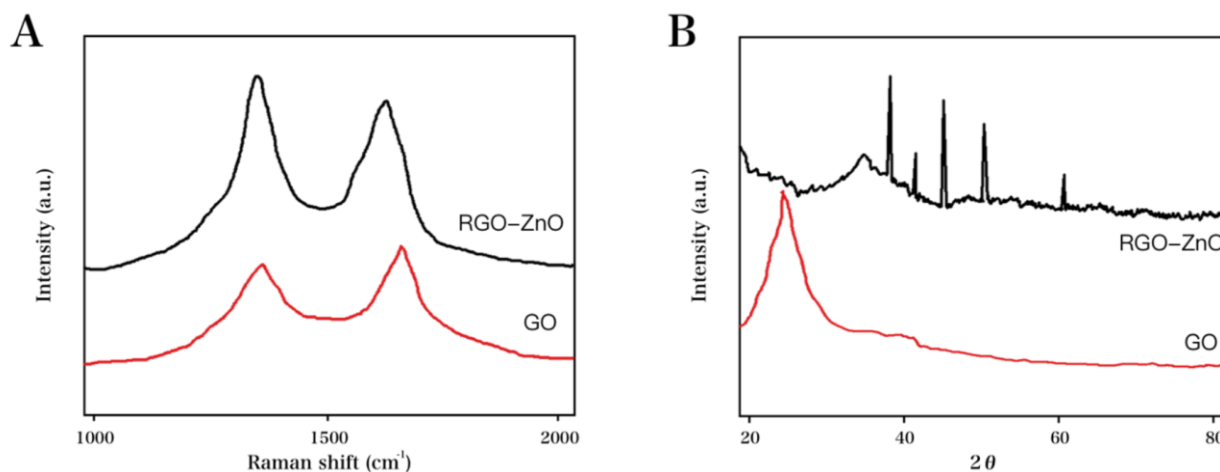


Figure 1. (A) Raman spectra and (B) XRD characterizations recorded for the GO and RGO-ZnO nanocomposite.

The analysis of the electrochemical performance of 0.5 mM HY was separately realized through cyclic voltammetry. Cyclic voltammetry (CV) was carried out to study the electrochemical performance of the bare GCE, ZnO-modified GCE, RGO-modified GCE and RGO-ZnO-coated GCE towards the detection of 1 mM CA, as shown in Fig. 2. At RGO-ZnO-modified GCE, no significant peaks were recorded without adding AD (Fig. 2). However, at the four different modified electrodes, obvious oxidization peaks can be observed for CA; the current responses were obtained as 0.0125, 0.0427, 0.0699 and 0.1271 mA for the bare GCE, ZnO-modified GCE, RGO-coated GCE and RGO-ZnO-modified GCE, respectively (oxidation potentials: 0.51, 0.45, 0.42 and 0.35 V, respectively). Obviously, the RGO-ZnO-modified GCE showed an increased peak current together with a decreased peak potential, which suggests that the proposed electrode was more highly electrocatalytically active towards the detection of CA compared to the other three electrodes. The enhancement probably resulted from the large surface-to-volume ratio, high electrical conductivity, favourable biocompatible, excellent catalytic ability and surface reaction activity.

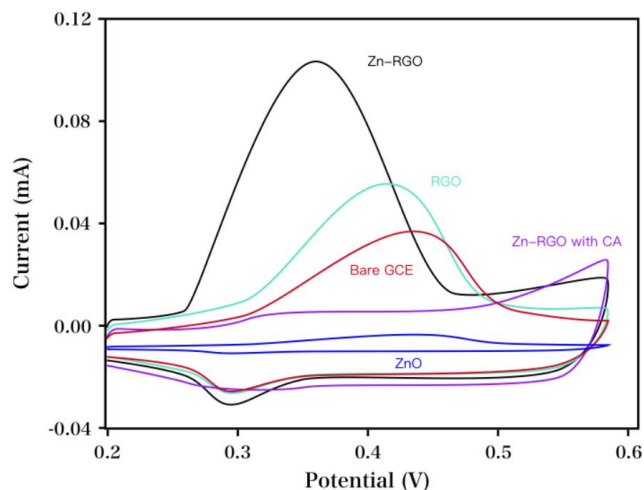


Figure 2. CV recorded for the bare GCE, ZnO-modified GCE, RGO-modified GCE, and RGO-ZnO-modified GCE in 0.1 M PBS before and after the addition of 1 mM CA (scan rate: 50 mV/s).

We continued to study the influence of the scan rate on the electrochemical performance of the RGO-ZnO-coated GCE towards the electrocatalytic oxidation of CA. At the proposed electrode, CVs were recorded over a range of 20 - 260 mV/min after adding 1 mM CA. The oxidation potential shifted to a more positive potential as the scan rate increased, meanwhile an increase in the peak current was also observed. This observation can be explained by the kinetic limitation of the reaction between the redox sites of the RGO-ZnO and the CA, as confirmed by the previous literature [25, 26]. Therefore, the redox of CA at the RGO-ZnO surface was controlled by diffusion. As seen from Fig. 5B, the peak current was linearly related to the square root of the scan rate, with a linear regression equation of I_{pa} (μA) = $17.71v^{1/2} - 2.38$ ($R^2 = 0.994$), which indicated that the electrode surface reaction was controlled by the mass transfer.

The linear regression was described in terms of the logarithm of the scan rate and the peak potentials by the following equation: E_{pa} (V) = $0.09213 \log v + 0.23966$ ($R^2 = 0.988$). Based on this linear equation, the calculation of the number of electrons participating in the reaction could be described by Laviron's equation [27, 28] as follows:

$$E_p = E^{\circ} + (2.303RT / \alpha nF) \log(RTk_o / \alpha nF) + (2.303RT / \alpha nF) \log v$$

where E° refers to the formal redox potential; R represents the gas constant; α denotes the electron transfer coefficient; F refers to the Faraday's constant; and k_o represents the standard heterogeneous rate constant of the reaction. The slope of E_p against $\log v$ is 0.09547, and the value of αn can be easily obtained as 0.5417. Therefore, the calculation of the α value is described as follows:

$$E_{p/2} - E_p = 1.875(RT / \alpha F)$$

where α was calculated to be 0.7474, from which the total number of electrons participating in the oxidation of uric acid was calculated to be 2; this figure was consistent with that of previously published literature [25, 29, 30].

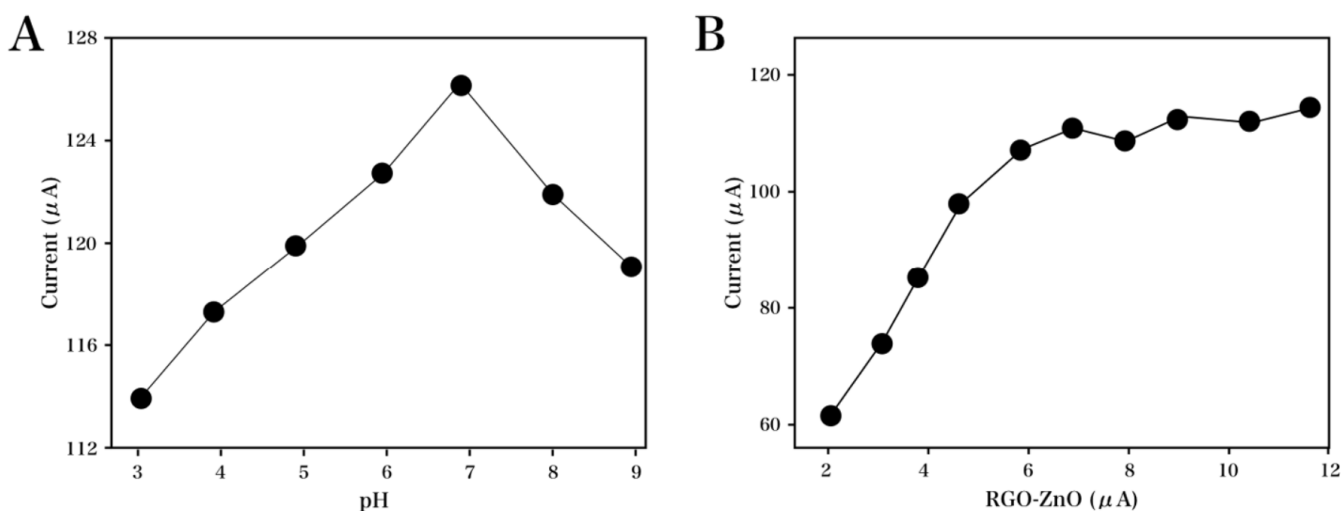


Figure 3. Plots of I_{pa} against (A) PBS pH and (B) the amount of modifier for the detection of CA.

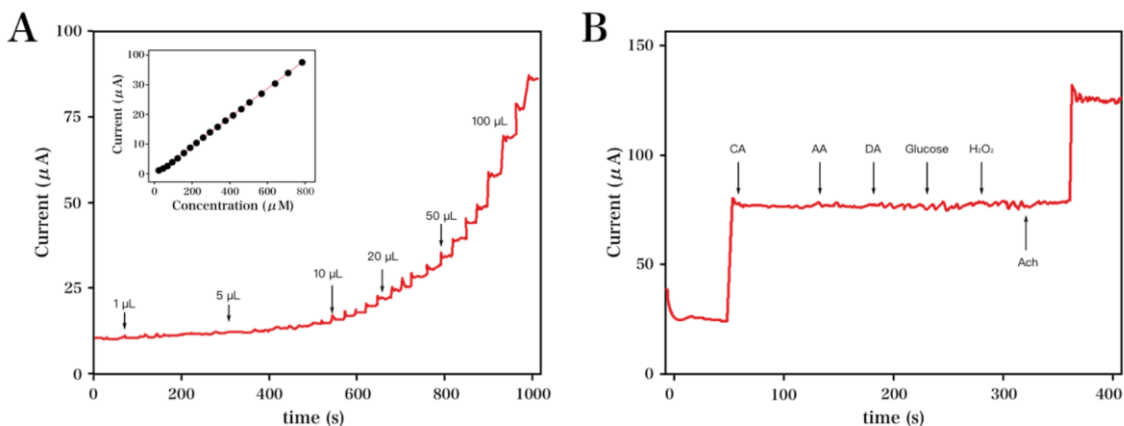


Figure 4. (A) Amperometric response obtained at the RGO-ZnO modified GCE at 0.38 V after successively adding uric acid into the PBS. Inset: Magnification of the current responses over a range of 1 - 10 μM . (B) Amperometric current response obtained at the RGO-ZnO-modified GCE to the addition of 0.5 mM UA, 5 mM AA, 5 mM CA, Ach, glucose, and H_2O_2 (operating potential: 0.38 V).

The pH effect on the CA detection was also investigated. As the pH increased over a range of 3 - 7, a gradual increase in the peak current was observed (Fig. 3A). In the case of pH 7, the peak current reached its maximal value at 127.1 μA . This was followed by a decrease at higher pH values. Thus, we optimized the pH as 7. Moreover, the neutral condition is also favourable for biological determinations [31-33].

Another important factor that can affect the anodic peak current of CA is the modifier amount. With the increase in the modifier amount over a range of 2 - 8 μL , an obvious increasing trend can be observed in the peak current (Fig. 3B). The current response slightly decreased at higher modifier amounts, which possibly resulted from the prolonged time for the electrons of CA to transfer through the thick RGO-ZnO film.

The characteristic amperometric response of our proposed biosensor after successively adding CA was recorded in Fig. 4A. Within 7 s, a stable state was recorded for the as-prepared biosensor, which indicated a fast response to the detection of CA. Over a range of 1 - 800 μM , the current response was found to be linearly related to the concentration of CA, as shown in the following linear regression equation: $I (\mu\text{A}) = 0.1124 C(\mu\text{M}) + 16.741$ ($R^2 = 0.9982$). The limit of detection (LOD) was obtained as 0.322 μM ($S/N=3$). To allow for comparisons with previous reports, the characteristics of the different electrochemical sensors for creatinine are summarized in Table 1.

Table 1. Comparison of the major characteristics of electrochemical sensors used for the detection of CA.

Electrode	Linear detection range	Detection limit	Reference
Fullerene-functionalized carbon nanotubes/ionic liquid	0.07–30.0 μM	0.01 μM	[37]
Fluorine-doped SnO_2	2–600 μM	0.7 μM	[38]
Poly(methylvinyl ether)/RGO	5 - 200 μM	1.6 μM	[39]
RGO-ZnO modified GCE	1 - 800 μM	0.322 μM	This work

For comparison purposes, an HPLC method and the RGO-ZnO-modified GCE were used to determine CA in serum samples (Table 2). The result showed that the proposed electrochemical method had a similar performance compared to that of the HPLC method.

Table 2. Detection of hydrazine in tap water using the proposed electrochemical method and GC-MS.

Serum sample	Added (μM)	HPLC (μM)	ZnO NPs/GCE (μM)	RSD (%)
1	10	9.78	9.81	5.66
2	100	104.51	103.01	4.23
3	200	195.21	202.35	4.19
4	300	288.51	296.32	2.01

We investigated the effects of several physiological interfering agents to study the selectivity of our developed biosensor. After the addition of CA and several possible interfering agents, including AA, UA, glucose, H_2O_2 and Ach, the characteristic response of the proposed electrode was recorded in Fig. 4B. After the addition of 5 mM AA, UA, glucose, H_2O_2 and Ach, we observed no apparent variation in the current response, which suggested the high selectivity of our developed biosensor to CA even after adding interfering agents in excess of up to 10-fold.

4. CONCLUSIONS

In the present study, a facile one-pot hydrothermal treatment was employed for the preparation of a state-of-the-art RGO-ZnO nanocomposite. Furthermore, the GCE modified by this nanocomposite was successfully applied with high selectivity towards the detection of CA. Therefore, this simple strategy can be used to analyse human urine from DA healthy volunteers and patients with high accuracy.

References

1. A.Kumar, J.P. Hart and D.V. Mccalley, *Journal of Chromatography A*, 1218 (2011) 3854.
2. D.M. Omiatek, A.J. Bressler, A.S. Cans, A.M. Andrews, M.L. Heien and A.G. Ewing, *Scientific Reports*, 3 (2013) 1447.
3. M. Tsunoda, C. Aoyama, S. Ota, T. Tamura and T. Funatsu, *Analytical Methods*, 3 (2011) 582.
4. I.A. Ges, K.P.M. Currie and F. Baudenbacher, *Biosensors & Bioelectronics*, 34 (2012) 30.
5. J.J. Colleran and C.B. Breslin, *Journal of Electroanalytical Chemistry*, 667 (2012) 30.
6. M. Rafiee and L. Khalafi, *Electrochimica Acta*, 55 (2010) 1809.
7. J.J. Colleran and C.B. Breslin, *Journal of Electroanalytical Chemistry*, 667 (2012) 30.
8. J.A. Ribeiro, P.M. Fernandes, C.M. Pereira and F. Silva, *Talanta*, 160 (2016) 653.
9. M. Young, W. Pan, J. Wiesner, D. Bullough, G. Browne, G. Balow, S. Potter, K. Metzner and K. Mullane, *Drug Development Research*, 32 (2010) 19.
10. L. Liu, Q. Li, N. Li, J. Ling, R. Liu, Y. Wang, L. Sun, X.H. Chen and K. Bi, *Journal of Separation Science*, 34 (2011) 1198.

11. M. Denegri, R. Bongianino, F. Lodola, S. Boncompagni, V.C.D. Giusti, J.E. Avelinocruz, N. Liu, S. Persampieri, A. Curcio and F. Esposito, *Circulation*, 129 (2014) 2673.
12. J.H. Henriksen, H. Ringlarsen and N.J. Christensen, *Clinical Physiology & Functional Imaging*, 8 (2010) 203.
13. D.S. Goldstein, I.J. Kopin and Y. Sharabi, *Pharmacology & Therapeutics*, 144 (2014) 268.
14. K. Jodko and G. Litwinienko, *Postepy Biochemii*, 56 (2010) 248.
15. TNatsukawa, TTanigawa and MTakeda, *Biological Rhythm Research*, 27 (2010) 138.
16. T. Kanamori, T. Funatsu and M. Tsunoda, *The Analyst*, 141 (2016) 2568.
17. D. Quan and W. Shin, *Electroanalysis*, 16 (2010) 1576.
18. X. Xu, H. Zhang, H. Shi, C. Ma, B. Cong and W. Kang, *Analytical Biochemistry*, 427 (2012) 10.
19. L. Fu, A. Wang, G. Lai, C.-T. Lin, J. Yu, A. Yu, Z. Liu, K. Xie and W. Su, *Microchimica Acta*, 185 (2018) 87.
20. L. Fu, A. Wang, G. Lai, W. Su, F. Malherbe, J. Yu, C.-T. Lin and A. Yu, *Talanta*, 180 (2018) 248.
21. L. Fu, K. Xie, H. Zhang, Y. Zheng, W. Su and Z. Liu, *Coatings*, 7 (2017) 232.
22. T. Yoshitake, J. Kehr, S. Yoshitake, K. Fujino, H. Nohta and M. Yamaguchi, *Journal of Chromatography B Analytical Technologies in the Biomedical & Life Sciences*, 807 (2004) 177.
23. Y. Umegae, H. Nohta, M. Lee and Y. Ohkura, *Chemical & Pharmaceutical Bulletin*, 38 (1990) 2293.
24. X. Zhang, D. Zhang, Y. Chen, X. Sun and Y. Ma, *Chinese Science Bulletin*, 57 (2012) 3045.
25. M. Ahmad, E. Ahmed, Z.L. Hong, N.R. Khalid, W. Ahmed and A. Elhissi, *J. Alloy. Compd.*, 577 (2013) 717.
26. M. Ahmad, E. Ahmed, Z.L. Hong, J.F. Xu, N.R. Khalid, A. Elhissi and W. Ahmed, *Appl. Surf. Sci.*, 274 (2013) 273.
27. C. Xu, X. Wang and J. Zhu, *J Phys Chem C*, 112 (2008) 19841.
28. D. Oukil, L. Benhaddad, R. Aitout, L. Makhoulfi, F. Pillier and B. Saidani, *Sensors and Actuators B: Chemical*, 204 (2014) 203.
29. Y. Wei, M. Li, S. Jiao, Q. Huang, G. Wang and B. Fang, *Electrochimica Acta*, 52 (2006) 766.
30. E. Laviron, *J. Electroanal. Chem.*, 52 (1974) 355.
31. E. Laviron, *J. Electroanal. Chem.*, 101 (1979) 19.
32. X. Cao, Y. Xu, L. Luo, Y. Ding and Y. Zhang, *Journal of Solid State Electrochemistry*, 14 (2010) 829.
33. H. Manjunatha, D.H. Nagaraju, G.S. Suresh and T.V. Venkatesha, *Electroanalysis*, 21 (2009) 2198.
34. J.A. Ribeiro, P.M. Fernandes, C.M. Pereira and F. Silva, *Talanta*, 160 (2016) 653.
35. L. Chen, X. Zhu, J. Shen and W. Zhang, *Analytical and bioanalytical chemistry*, 408 (2016) 4987.
36. S. Chitravathi and N. Munichandraiah, *Journal of The Electrochemical Society*, 162 (2015) B163.
37. M. Mazloun-Ardakani and A. Khoshroo, *Electrochemistry Communications*, 42 (2014) 9.
38. C. Ramírez, M.A. Del Valle, M. Isaacs and F. Armijo, *Electrochimica Acta*, 199 (2016) 227.
39. R. Han, J. Ma and L. He, *International Journal of Electrochemical Science*, 12 (2017) 10338